Stochastic model reduction for polynomial chaos expansion of acoustic waves using proper orthogonal decomposition

Nabil El Moçayd[a,*], M. Shadi Mohamed[b], Driss Ouazar[a], Mohammed Seaid[c]

[a] *International Water Research Institute, University Mohammed VI Polytechnic, Benguerir, Morocco*
[b] *School of Energy, Geoscience, Infrastructure and Society, Heriot-Watt University, Edinburgh EH14 4AS, UK*
[c] *Department of Engineering, University of Durham, South Road, Durham DH1 3LE, UK*

Abstract

We propose a non-intrusive stochastic model reduction method for polynomial chaos representation of acoustic problems using proper orthogonal decomposition. The random wavenumber in the well-established Helmholtz equation is approximated via the polynomial chaos expansion. Using conventional methods of polynomial chaos expansion for uncertainty quantification, the computational cost in modelling acoustic waves increases with number of degrees of freedom. Therefore, reducing the construction time of surrogate models is a real engineering challenge. In the present study, we combine the proper orthogonal decomposition method with the polynomial chaos expansions for efficient uncertainty quantification of complex acoustic wave problems with large number of output physical variables. As a numerical solver of the Helmholtz equation we consider the finite element method. We present numerical results for several examples on acoustic waves in two enclosures using different wavenumbers. The obtained numerical results demonstrate that the non-intrusive reduction method is able to accurately reproduce the mean and variance distributions. Results of uncertainty quantification analysis in the considered test examples showed that

*Corresponding author
Email addresses: nabil.elmocayd@um6p.ma (Nabil El Moçayd), m.s.mohamed@hw.ac.uk (M. Shadi Mohamed), driss.ouazar@um6p.ma (Driss Ouazar), m.seaid@durham.ac.uk (Mohammed Seaid)

the computational cost of the reduced-order model is far lower than that of the full-order model.
Keywords: Proper orthogonal decomposition, Polynomial chaos expansion, Uncertainty quantification, Stochastic Helmholtz equation, Acoustic waves.

---

1. Introduction

Advancements in numerical modelling of wave propagation allowed engineers to develop applications in many fields. Ranging from global positioning systems [1] and mobile phones [2, 3] to medical instrumentation [4, 5] and subsurface imaging [6, 7], the numerical tools provide a precious help for stakeholders in order to make relevant decisions [8, 9]. However, despite the great efforts made to model waves, it is often the case that numerical responses are simulated with ubiquitous uncertainties [8, 9]. There are many inevitable sources of uncertainty for which a modeler should deal with during the numerical simulation. For example, it is often the case that the subsurface soil properties in geophysics are identified with uncertainty which will then be reflected in identifying the problem wavenumber or boundary conditions, compare [10, 11] among others. Covering both physical approximation and numerical parametrization, all these necessary assumptions lead to generation of uncertain simulations. Consequently, many works nowadays focus on quantifying the uncertainty encompassed in a numerical model, compare [12, 13, 14, 15].

In practice, Uncertainty Quantification (UQ) can be carried out using either the well-established intrusive techniques [16, 17, 18] or non-intrusive procedures [19, 20, 21]. The first approach needs the modification of the deterministic numerical algorithm whereas, the second approach uses the numerical model as a black box. Since accurate numerical methods for solving the Helmholtz equation are still a challenging research field [22] and in order to develop a general framework for UQ in computational acoustics, the focus in the present study is on the non-intrusive approach. Stochastic simulations remain the most popular techniques for uncertainty quantification. Indeed, the ensemble-based methods

[23, 24, 25, 26] are very easy to implement and more importantly they do not need to change the main model. The basic idea of the ensemble-based methods remains in the central limit theorem, see for example [27]. The theorem states that a large number of random variable samples well defined in a probabilistic space ensures its convergence in distribution according to the associated probability density function. In fact, the well-known Monte-Carlo (MC) sampling methods are a class of powerful tools because they ensure the convergence. However, in order to guarantee convergence, the MC methods require a large number of simulations to be performed. Therefore, many efforts have been deployed in order to achieve efficient methods for the uncertainty quantification (UQ), see for instance [28, 12]. In order to outperform the classical MC simulations, these new methods have to be at least as accurate as MC methods to estimate the uncertainty and in addition they should require less computational times. One leading idea in the UQ applications is to replace the expensive full model by a meta-model, also known as surrogate model [29]. The aim here is to mimic the behavior of the model while requiring less computational time to simulate the response. Hence, different meta-models have been developed in the community but Kriging and Polynomial Chaos Expansion (PCE) are considered to be the most used to treat UQ, see [30, 31, 32, 33, 34, 35] among others. In the current work, accounting for the complex physics in acoustics, the PCE is preferred over the Kriging in order to ensure convergence as stated in [33].

Spectral decomposition is widely used in numerical simulation of many practical problems. In the probabilistic context, it consists in projecting a random variable (response of a model) in a suitable basis of finite dimensions. The theory behind PCE lies on building the base from a set of orthogonal polynomials. Therefore, defining a reduced model from this technique is based on calculating the polynomial coefficients. An intuitive method for calculating these coefficients is to replace the model response by its approximation in the partial differential equations governing the problem under study whereas, the coefficients are thus calculated directly by the Galerkin method. These methods have been presented for the first time to solve problems in structural mechanics

with random input variables in [36]. It should be noted that this method is called intrusive because it requires to modify the existing computer program. Alternatively, non-intrusive methods consist of using the computer code as a black box without amendments. In this case, obtaining the response solutions can only be carried out through model evaluations. These methods make it possible to obtain a polynomial approximation from an ensemble-based technique. It was first used in [36] for resolving the uncertainty propagation as an alternative to MC methods and its application is based on the corollary of Cameron-Martin theorem [37]. In addition, the work presented in [38] made it possible to generalize the previous study on the chaos polynomials for other classes of probability distributions than the Gaussian law adopting the Askey scheme from [39] known by generalized Polynomial Chaos (gPC) and widely used in the literature. For the sake of simplicity through this paper we will refer to PCE for gPC. Several studies have also been published in the literature to illustrate the efficiency of PCE in the context of UQ, sensitivity analysis and also as a powerful tool to accelerate inverse problems such as data assimilation, see for instance [40, 15, 41] and further references are therein.

In the framework of developing meta-models to reduce the computational cost in the UQ, many efforts have been engaged in order to overcome the challenges presented by the advanced numerical models. This is mainly because the construction time required for PCE increases exponentially with the stochastic dimension, see for example [42, 43] and further references are therein. One of the main challenges was to overcome the problem of stochastic dimensions in the model input parameters. For example, authors in [44] introduced the adaptive sparse PCE to tackle this problem. The idea is to use a least angle regression as defined in [45], to estimate the PCE based on a regression method. Another study presented in [46] combines Kriging and PCE to introduce a new meta-model. This technique allows to take into account the global and local behaviors of UQ. However, few studies focused on the physical dimension of the output variables. In fact in many studies, when an UQ algorithm is implemented over a numerical model while the output solution is a physical field discretized in a

mesh, the method needs computation of the PCE in every node of the mesh, see for example [40, 47, 48]. For these situations, the numerical resolution of complex acoustic features requires fine meshes which results in highly computational costs. It should also be stressed that the physical outputs are stochastic processes with spatial or/and temporal correlations rather than stochastic variables. Thus, the uncertainty displayed over this process is not even neither in space nor in time. Different outputs are expected for each nodal point in the computational mesh and at every time step in the time interval. Therefore, there is a need to develop less time-consuming methodologies in order to quantify the uncertainty when the output is a stochastic process. In addition, dimension reduction is a common tools needed for UQ and nowadays each model needs a high number of input parameters to run. As all these parameters could lead to ubiquitous uncertainty, one strategy to reduce the computational burden, is to fix the parameters to which the uncertainty of the response is insensitive. For instance, these methods have been considered in [49] using the method of moments and in [47] using the sparse polynomial decomposition. However, when the uncertain input in the model is a vector-based parameter, neglecting one of its components may deteriorate the uncertainty described by this vector and consequently it may fail to capture the correct physical features of the numerical solution.

One way used in the literature to alleviate this problem consists of using the Karhunen-Loève decomposition, see for example [50, 51, 52]. Furthermore, for high dimensions in the model output dimension, other different techniques could be adopted including the Principal Component Analysis (PCA) [53], the Proper Generalized Decomposition (PGD) [54], and the Proper Orthogonal Decomposition (POD) [55] among others. It should be stressed that the main idea on these techniques relies in the fact that uncertainty features are described in the response of random vectors with few non-physical variables. The statistical interests are obtained using resampling of the new surrogate model. Therefore, due to the complex physical features in the Helmholtz equation for which the acoustic response exhibits steep gradients and localized structures, the POD is

implemented in the current study.

In this work, a non-intrusive reduced-order technique is developed and applied to the two-dimensional propagation of acoustic waves. We consider the wave model in the frequency domain and the governing equation reduces to a stochastic Helmholtz problem. It is well known that to increase the contribution and reliability of computational acoustics in design process of industrial equipments, it is necessary to quantify the effects of uncertainties on the system performance. As a numerical solver we implement the finite element method for the Helmholtz equation to compute the complex solution. Our main focus in the current study is on uncertainty associated with the wavenumber in acoustic waves. We therefore eliminate different sources of error in the approximations made by the numerical solver to try to quantify only the uncertainty associated with the wavenumber. Usually the acoustic signals measurements are affected by random environmental factors, which will negatively affect the certainty of the measured results [56]. Quantifying the effect of such uncertainties is important to validate the deterministic problem solution. The main focus is on the UQ in the simulation of acoustic potential resulting from uncertain wavenumbers related to uncertain frequency and celerity of the waves under study. We investigate the use of a proper orthogonal decomposition (POD) to reduce the dimensionality of the problem outputs.

To assess the performance of the proposed methodology, several test examples are simulated using different wavenumbers. We also perform a comparison between the proposed approach and a class of massive MC simulations in terms of mean and variance fields. The remaining of this paper is organized as follows. In Section 2 we present details of the mathematical formulation and the problem under investigation. The model reduction methodology along with PCE and POD techniques are described in Section 3. Section 4 outlines the performance of the proposed methods using several applications in acoustics. Finally, concluding remarks are included in Section 5.

2. Finite element method for modelling acoustic waves

In the present work we are interested in the finite element method solution of the time-harmonic exterior wave equation. The flexibility of the finite element method in dealing with complex geometries and material heterogeneity, makes it a popular option for solving this type of problems, see for example [57, 58, 59, 60, 61]. The solution is relevant to computational acoustics among other applications, [62, 63, 64]. The finite element method is also well studied in the literature for this type of applications, however, for completeness we briefly introduce the finite element formulation of the problem in this section. Hence, we consider an open bounded domain Ω in $\mathbb{R}^2$ where waves can propagate to infinity. To solve the problem with the finite element method we need to truncate the domain at some boundary $\partial\Omega$. The wave potential $u(x, y) \in H^1(\Omega)$ can then be defined as a function that satisfies the well-established Helmholtz equation

$$\Delta u + \kappa^2 u = 0, \quad \text{in} \quad \Omega, \tag{1}$$

where $\kappa > 0$ is the wave number, Δ the Laplace operator and $H^1(\Omega)$ the standard Sobolev space. Furthermore, we impose a Robin-type boundary condition on $\partial\Omega$ as

$$\nabla u \cdot \mathbf{n} + \mathrm{i}\kappa u = g, \quad \text{on} \quad \partial\Omega, \tag{2}$$

where $\mathrm{i}=\sqrt{-1}$, $g(x, y)$ is the imposed boundary function, ∇ the gradient vector operator and $\mathbf{n}$ the outward unit normal to $\partial\Omega$. The considered boundary-value problem is defined by the equations (1) and (2). In this study we concentrate on the impact of the uncertainty in the wavenumber κ on the finite element solution of the the problem (1)-(2). Therefore, to eliminate numerical errors of approximating radiation boundary conditions we avoid solving a full exterior problem. Furthermore, the boundary condition (2) is used to impose the analytical solution of the deterministic problem on the domain boundary $\partial\Omega$. Thus, we also eliminate numerical errors resulting from approximating the geometry.

To recover the solution $u(x, y)$ in Ω using the finite element method, we first multiply the equation (1) with a weighting function $w(x, y) \in H^1(\Omega)$, integrate

over Ω and then use the divergence theorem, which yields

$$\int_{\Omega} \left(-\nabla w \cdot \nabla u + \kappa^2 w u\right) d\Omega + \int_{\Gamma} w \nabla u \cdot \mathbf{n}\, d\Gamma = 0. \tag{3}$$

Substituting the boundary condition (2) into this form we obtain the following weak formulation

$$\int_{\Omega} \left(\nabla w \cdot \nabla u - \kappa^2 w u\right) d\Omega + \mathrm{i}\kappa \int_{\Gamma} w u\, d\Gamma = \int_{\Gamma} w g\, d\Gamma. \tag{4}$$

Using the finite element method, it is possible to recover an approximation for $u(x, y)$ by solving the equation (4). Hence, we first discretize (4) by meshing the domain Ω into a set of elements T_i

$$\mathcal{T}_h = \{T_1, T_2, \ldots, T_N\}, \tag{5}$$

with each element T_i is a sub-domain of Ω and a union of all elements forms the computational domain $\Omega_h = \bigcup_{T_i \in \mathcal{T}_h} T_i$. We also assume that the standard finite element requirements are satisfied by all the elements and h refers to the characteristic element size. Hence, we define a discrete space $W_h \subset H^1(\Omega_h)$ by

$$W_h = \left\{ w \in C^0(\Omega_h) : \quad w\big|_{T_i} \in P(T_i) \qquad \forall\, T_i \in \mathcal{T}_h \right\}, \tag{6}$$

where $P(T_i)$ is the space of linear polynomials defined on the element T_i. The solution approximation space W_h has a finite number of dimensions M which is the number of basis functions in the space. Thus, the solution u can then be approximated using the finite element method as a linear combination of these basis functions $\mathcal{N}_j$ such as

$$u(x, y) \approx u_h = \sum_{j=1}^{M} u_j \mathcal{N}_j(x, y), \tag{7}$$

where u_j are the values of u_h at the elemental nodes. Using the basis functions $\mathcal{N}_j$ to also replace the weighting function in the weak formulation (4), we can rewrite the weak formulation as a summation over the discretized domain

$$\sum_{j=1}^{M} \left(\int_{\Omega} \left(\nabla \mathcal{N}_j \cdot \nabla \mathcal{N}_i - \kappa^2 \mathcal{N}_j \mathcal{N}_i\right) d\Omega + \mathrm{i}\kappa \int_{\Gamma} \mathcal{N}_j \mathcal{N}_i\, d\Gamma \right) u_j = \int_{\Gamma} \mathcal{N}_i g\, d\Gamma. \tag{8}$$

The integration over Ω in the discrete weak formulation is performed element by element using the well-established Gauss quadratures. Linear basis functions on quadrilateral elements are selected in the current work. This results in a linear system of algebraic equations as

$$\mathbf{A}\mathbf{x} = \mathbf{b}, \tag{9}$$

where $\mathbf{A}$ being a sparse symmetric $M \times M$ matrix while the M unknown nodal values of the solution u_j are represented in the vector $\mathbf{x}$. The entries of the matrix $\mathbf{A}$ and the vector $\mathbf{b}$ in this linear system (9) are given by

$$A_{j,i} = \int_\Omega \left(\nabla \mathcal{N}_j \cdot \nabla \mathcal{N}_i - \kappa^2 \mathcal{N}_j \mathcal{N}_i \right) \, d\Omega + \mathrm{i}\kappa \int_\Gamma \mathcal{N}_j \mathcal{N}_i \, d\Gamma,$$

and

$$b_j = \int_\Gamma \mathcal{N}_i g \, d\Gamma,$$

respectively. It should be noted that the basis functions preserve the Kronecker delta property *i.e.* take a value of one at one node and zero at any other node. Hence, the associated matrix $\mathbf{A}$ is a sparse matrix. The linear system (9) is solved with a direct solver using a general triangular factorization computed by the Gaussian elimination with partial pivoting. Notice that, if a high wavenumber is considered in the acoustic problem, a large number of basis functions is needed to have a proper approximation for the considered boundary-value problem. This may lead to the matrix $\mathbf{A}$ becoming ill-conditioned. To avoid this situation in the current study, we concentrate on acoustic wave problems with relatively low wavenumbers.

3. Uncertainty quantification for the stochastic process

We describe the general methodology with an eye towards solving stochastic acoustic waves. We briefly discuss techniques used for polynomial chaos expansions and stochastic proper orthogonal decomposition. Details on the application of these tools for quantifying uncertainties in acoustic waves are also

presented in this section. Accounting for stochastic input parameter $\boldsymbol{\zeta}$ in (1)-(2), the stochastic Helmholtz problem we consider in the present study reads

$$\begin{aligned} \Delta \boldsymbol{U} + \kappa^2 \boldsymbol{U} &= 0, \quad \text{in} \quad \Omega, \\ \nabla \boldsymbol{U} \cdot \mathbf{n} + \mathrm{i}\kappa \boldsymbol{U} &= g, \quad \text{on} \quad \partial\Omega, \end{aligned} \tag{10}$$

where $\boldsymbol{U}(x, y, \boldsymbol{\zeta})$ is the stochastic wave potential, $\kappa(\boldsymbol{\zeta})$ the stochastic wave number and $g(x, y, \boldsymbol{\zeta})$ the stochastic boundary function.

3.1. Polynomial chaos expansions

Polynomial chaos expansion has been intensively used as a surrogate model in the context of uncertainty quantification. It aims to reproduce the global behavior of a simulation following a polynomial decomposition. The multivariate polynomials that form the basis are chosen according to the probability density function of the supposed stochastic input variables as defined for example in [65, 38]. In the present study, the decomposition of the simulation response $\boldsymbol{U}$ in the Cartesian coordinates (x, y) is given by

$$\boldsymbol{U}(x, y, \boldsymbol{\zeta}) = \sum_{i \in \mathbb{N}} \alpha_i(x, y) \Psi_i(\kappa(\boldsymbol{\zeta})), \tag{11}$$

where $\boldsymbol{\zeta}$ is the vector containing all the stochastic input parameters in the stochastic space, α_i are the spectral coefficient of the decomposition to be determined hereinafter, and $(\Psi_i)_{i \geq 0}$ are the orthogonal polynomial basis. Note that, because of the stochastic nature of the input variable $\kappa(\boldsymbol{\zeta})$, the response $\boldsymbol{U}$ has also a stochastic component assumed to be of finite variance. In practice, the sum in (11) is truncated to a finite series as

$$\boldsymbol{U}(x, y, \boldsymbol{\zeta}) \approx \sum_{i \in \mathcal{I} \subset \mathbb{N}} \alpha_i(x, y) \Psi_i(\kappa(\boldsymbol{\zeta})). \tag{12}$$

The determination of a PCE is therefore conditioned by the estimation of the spectral coefficients α_i. There are many methods used in the literature to achieve this step and we refer the reader to [13, 66, 67] for a deep discussion on these methodologies. For the sake of simplicity and without loss of generalities, only

the regression method is considered in the present work and one can use the most efficient sparse decomposition when the stochastic dimension is very high, see for example [44]. It should be stressed that the well-established quadrature techniques are not considered in the current study because they can not be used to build the POD modes.

The regression method is based on solving a least-square (LS) minimization problem in some ℓ_2-norm to estimate the coefficients α_i, see for instance [68, 30]. In practice, we begin by defining an error $\boldsymbol{\epsilon}$ as the distance between the model and the PCE for a finite set of randomly sampled input variables of size N_{ls} such that

$$\boldsymbol{\epsilon} = \boldsymbol{U}(x, y, \boldsymbol{\Xi}) - \sum_{i \in \mathbb{N}} \alpha_i(x, y) \Psi(\kappa(\boldsymbol{\Xi})) \equiv \mathcal{U} - \boldsymbol{\alpha}^\top \boldsymbol{\Psi}, \tag{13}$$

where $\boldsymbol{\Xi} = [\boldsymbol{\zeta}^{(1)}, \ldots, \boldsymbol{\zeta}^{(N_{ls})}]^\top$ is the set of realizations for the stochastic input variables $\boldsymbol{\zeta}$, and $\mathcal{U} = [\boldsymbol{U}^{(1)}, \ldots, \boldsymbol{U}^{(N_{ls})}]^\top$ is the vector of associated model outputs. We also define $\boldsymbol{\alpha} = [\alpha_0, \ldots, \alpha_{N_{PC}-1}]^\top$ as the vector of the $N_{PC} = Card(\mathcal{I})$ unknown coefficients and $\boldsymbol{\Psi}$ is the matrix of size $N_{PC} \times N_{ls}$ assembling the values of all orthonormal polynomials at the stochastic input realizations values $\boldsymbol{\Psi}_{ik} = \Psi_i(\boldsymbol{\zeta}^{(k)})$, with $i = 0, 1, \ldots, N_{PC-1}$ and $k = 1, 2, \ldots, N_{ls}$. Estimating the set of coefficients $\boldsymbol{\alpha}$ following the ordinary least-square (13) which is equivalent to minimize the following function

$$\mathrm{J}(\boldsymbol{\alpha}) = \boldsymbol{\epsilon}^\top \boldsymbol{\epsilon} = \left(\mathcal{U} - \boldsymbol{\alpha}^\top \boldsymbol{\Psi}\right)^\top \left(\mathcal{U} - \boldsymbol{\alpha}^\top \boldsymbol{\Psi}\right), \tag{14}$$

leading to a standard well-known linear algebraic solution as

$$\boldsymbol{\alpha} = \left(\boldsymbol{\Psi}^\top \boldsymbol{\Psi}\right)^{-1} \boldsymbol{\Psi}^\top \mathcal{U}. \tag{15}$$

Here, the input space exploration is fulfilled thanks to a Monte-Carlo sampling-based approach as described in [69, 70] among others. The convergence of the MC simulations is monitored using a sensitivity analysis on the size of samples used as discussed in details for example in [71, 72, 73].

Note that, when dealing with numerical models with spatial or temporal dependency, the classical way consists on building a single surrogate model per

node of the mesh in the computational domain. It should also be mentioned that in many applications for acoustic waves, highly refined meshes are required to capture wave propagation at high wavelengths, see for instance [74]. This procedure leads to multiple decompositions to ensure the numerical convergence. As a result, uncertainty quantification becomes computationally very expensive not because of the stochastic dimensions but rather because of the spatial or temporal dimensions of the output variables. The infinite expansion describing PCE (11) converges with respect to the standard ℓ_2-norm known by the mean-squared convergence, see for example [13]. However, due to the errors of truncation and spectral coefficient estimation, the accuracy of such expansion must be evaluated in the same error norm. There are many different error metrics that allow to assess the accuracy of PCE, see [47, 13] among others. In the present work, all the PCEs are assessed using the *LOO* error. This method avoids integrating the model over another set of validation samples. It has been introduced in this context with the introduction of sparse PCE [30] and the *LOO* technique [75, 44] required the formulation of several surrogates. Each surrogate is built excluding one point out of the input sample and the accuracy of the surrogate is then calculated at this particular point. Following this theory, the error ϵ_{LOO} is defined by

$$\epsilon_{LOO} = \frac{\sum_{k=1}^{N_{ls}} \left(\boldsymbol{U}^{(k)} - \boldsymbol{U}^{(-k)} \right)^2}{\sum_{k=1}^{N_{ls}} (\boldsymbol{U}^{(k)} - \overline{\boldsymbol{U}})^2}, \tag{16}$$

where $\overline{\boldsymbol{U}}$ denotes the sample-averaged model simulations and $\boldsymbol{U}^{(-k)}$ stands for the evaluation of the PCE at $\boldsymbol{\zeta}^{(k)}$ when the surrogate has been built using an experimental design in which $\boldsymbol{\zeta}^{(k)}$ was excluded. In practice, the surrogate model is reconstructed once using all the samples and the error ϵ_{LOO} could be evaluated analytically as reported in [44]. In the present work, the determination of the optimal polynomial degree is performed using an iterative method. Here, a PCE is computed for different degrees varying from 1 to 20, then the optimal degree is determined based on the value of the corresponding ϵ_{LOO}. For a same

value of the error, the lowest value of the degree is retained.

3.2. Stochastic proper orthogonal decomposition

The proper orthogonal decomposition (POD) is a technique that allows a high-dimensional system to be approached by a low-dimensional one, compare [76] among others. This method consists in determining a basis of orthogonal eigenvalues representative of the simulated physics. The eigenvectors are obtained by solving the integral of Fredholm whereas, the kernel of this integral is constructed from a set of simulations constructed using an experimental design. The interesting property of this representation lies in the fact that the eigenfunctions associated with the problem are optimal in the sense of the energetic representation (as described later) which makes it possible to use them to construct a reduced representation of physics. The POD is used in uncertainty quantifications to reduce the size of a random vector at the output of the model. The uncertainty is therefore carried out over each direction defined by the eigenvectors λ_i. The idea is based on projecting the solution $\boldsymbol{U}$ of the model into a finite and orthonormal basis $\{\phi_i, i \in \mathcal{I}_{POD}\}$, where $\mathcal{I}_{POD}$ is a discrete finite set of indices. Thus, the process $\boldsymbol{U}(x, y, \boldsymbol{\zeta})$ is decomposed as

$$\boldsymbol{U}(x, y, \boldsymbol{\zeta}) = \sum_{i \in \mathcal{I}_{POD}} \lambda_i(\boldsymbol{\zeta}) \phi_i(x, y). \tag{17}$$

The estimation of $\{\phi_i,\ i \in \mathcal{I}_{POD}\}$ is performed by decomposing the spatial covariance matrix

$$\mathbf{C}(x, y) = \frac{1}{N_{ls}} \boldsymbol{U}\boldsymbol{U}^\top. \tag{18}$$

Indeed, the literature is rich of methodologies that aim to decompose a covariance matrix. One of the most known methods is the Singular Value Decomposition (SVD) algorithm. Furthermore, we define a POD-truncated error ϵ such as only the most k invaluable eigenvectors are retained as

$$\frac{\sum_{i=0}^{k} \widehat{\lambda}_i}{\sum_{i=0}^{N_{ls}} \widehat{\lambda}_i} > 1 - \epsilon, \tag{19}$$

where $\widehat{\lambda}_i$ is the mean value of $\lambda_i(\boldsymbol{\zeta})$. In summary, the stochastic POD procedure can be implemented using the following steps:

1. Define the covariance matrix (18).
2. Expand the matrix $\mathbf{C}$ using an SVD algorithm in order to determine λ_i and $\phi_i(x, y)$.
3. Retain only the first k eigenvalues and eigenvectors in the expansion using the condition (19).
4. Reconstruct the stochastic solutions $\boldsymbol{U}(x, y, \boldsymbol{\zeta})$ using (17).

It is worth mentioning that the selection of convergence criterion ϵ is problem dependent. The criterion choice of ϵ for test examples of present investigation is discussed in Section 4 where numerical examples are described.

3.3. The POD-PCE surrogate model

Once the stochastic POD is reconstructed, the eigenvalues are considered as random variables. This means that we can define a PCE for each eigenvalue following the same manner as described in the previous section on polynomial chaos expansions leaving the spatial dependence described by the eigenvectors $\phi_i(x, y)$ as

$$\lambda_i(\boldsymbol{\zeta}) = \sum_{j=0}^{N_{PC}} \gamma_j \Psi_j(\boldsymbol{\zeta}), \tag{20}$$

which reduces the equation (12) to

$$\boldsymbol{U}(x, y, \boldsymbol{\zeta}) = \sum_{i \in \mathcal{I}_{POD}} \left(\sum_{j=0}^{N_{PC}} \gamma_j \Psi_j(\boldsymbol{\zeta}) \right) \phi_i(x, y). \tag{21}$$

Figure 1 summarizes both algorithms that we consider in the present work for quantification of uncertainties in stochastic acoustics. Note that the classical way to deal with a problem of uncertainty quantification using the PCE is performed when a decomposition is achieved for each node in the computational mesh. This method is illustrated by steps 1, 2 and 3 in Figure 1. However as mentioned before, one method to alleviate the spatial distribution is to make a first reduction using the POD. This latter will help to separate the spatial

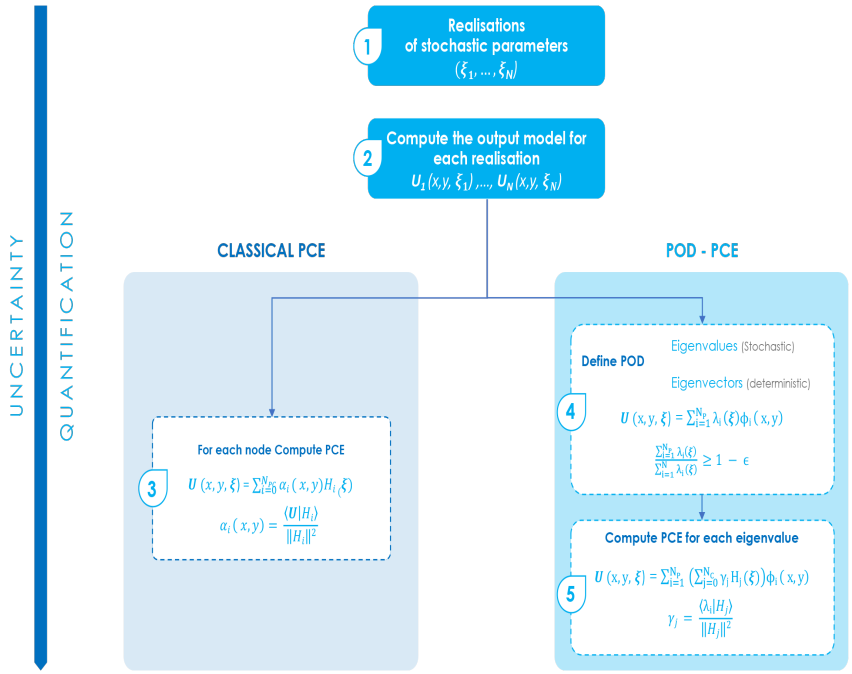

Figure 1: Schematic representation of the difference between flowcharts for the classical PCE based surrogate model and the POD-PCE based surrogate model.

dependence from the stochastic one as the stochasticity is included in the associated eigenvalues. Once the POD is carried out, only few eigenmodes are retained enabling to make less PCE than its conventional counterpart. This algorithm follows steps 1, 2, 4 and 5 in Figure 1. In the current work, a numerical evaluation of both methods is carried out using two test examples in computational acoustics. Special attention is given to the accuracy of the considered methods compared to the massive MC simulations (using 10^5 samples) for the quantities of interest in terms of mean and variance fields. In addition, a comparative study of efficiency in these techniques is also presented using CPU times required for each reconstruction. Notice that such approach has

also been tested in other cases. For example in [53], the PCE coefficients have been computed using the least angle regression over principal component eigenvalues which is similar to the POD approach. Another approach using the PCE of vector-valued response quantities has been reported in [77].

4. Numerical results and examples

In this section we assess the numerical performance of the proposed proper orthogonal decomposition for acoustics using two test examples on the Helmholtz problem (1)-(2). For each test example we present comparison results obtained using MC, PCE and POD-PCE methods for both the real and imaginary parts of the potential solution. In all our simulations, the value of the POD truncation criterion defined in section 3 is set to $\epsilon = 10^{-4}$.

4.1. Plane wave propagation

As a first test example we consider the problem of plane wave propagation in the squared domain $\Omega = [0,1] \times [0,1]$. Hence, we solve the two-dimensional Helmholtz problem (1)-(2) such that its exact deterministic solution is defined by

$$u(x,y) = \exp\Big(\mathrm{i}\kappa\big(x\cos\alpha + y\sin\alpha\big)\Big). \tag{22}$$

The boundary function g in (2) is derived from the analytical solution (22). Here, the wavenumber κ and the wave direction α are assumed to be stochastic parameters defined as

$$\kappa(\zeta_\kappa) = \overline{\kappa}\,(1 + CV\zeta_\kappa)\,, \qquad \alpha(\zeta_\alpha) = \overline{\alpha}\,(1 + CV\zeta_\alpha)\,, \tag{23}$$

where CV is the coefficient of variation associated to the physical values of the parameters $\kappa(\zeta_\kappa)$ and $\alpha(\zeta_\alpha)$, $\overline{\kappa}$ and $\overline{\alpha}$ are the mean values of κ and α, respectively. In (23), ζ_κ and ζ_α are the corresponding random variables which are supposed to follow the centered normal law $\mathcal{N}(0,1)$. In the results presented for this test example, the mean wave direction $\overline{\alpha} = \frac{\pi}{30}$ and two values of the mean wavenumber $\overline{\kappa}$ are selected. Here, the uncertainty is assessed for the quantities of interest over the acoustic potential $u(x, y, \zeta_\kappa, \zeta_\alpha)$.

Table 1: CPU times (in seconds) required by the PCE and POD-PCE methods for solving plane wave propagation problem using $\overline{\kappa} = 2\pi$. Numbers in parenthesis refer to the number of modes used in the POD-PCE method for a threshold of $\epsilon = 10^{-4}$. The results are obtained for an equivalent accuracy in both methods.

CV	PCE method	POD-PCE method
5 %	7311	41 (6)
10 %	7763	57 (8)
15 %	8330	61 (8)

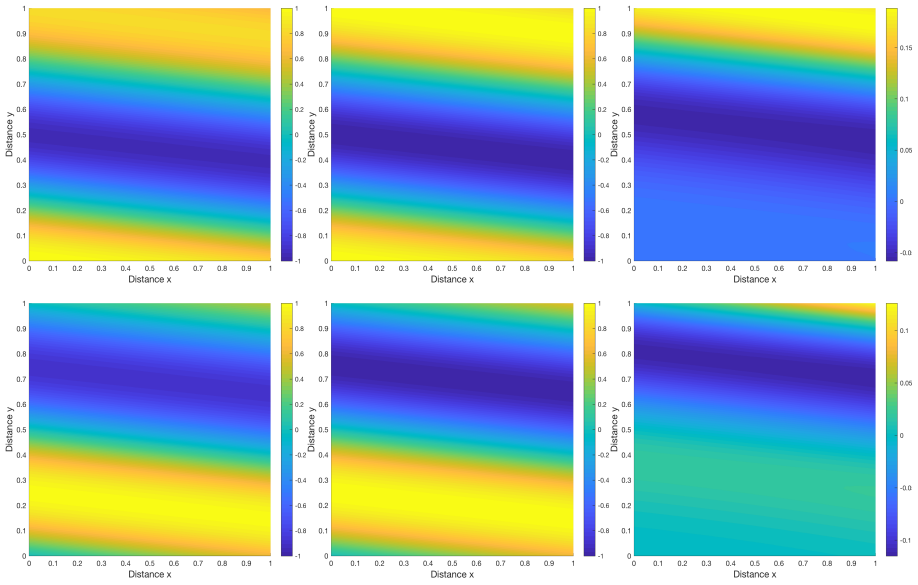

Figure 2: Mean wave potential $\overline{u(x, y, \zeta_\kappa, \zeta_\alpha)}$ obtained for the stochastic simulation (first column), the deterministic exact solution $u(x, y)$ (second column) and the difference between the two solutions (third column) obtained for plane wave propagation problem using $\overline{\kappa} = 2\pi$ and $CV = 10$ %. We present results for the real part (first row) and imaginary part (second row).

We first run the simulations using $\overline{\kappa} = 2\pi$ on a structured finite element mesh formed of 4-noded bilinear elements with a total number of 5740 elements and 5776 nodes. For the considered conditions, we present in Table 1

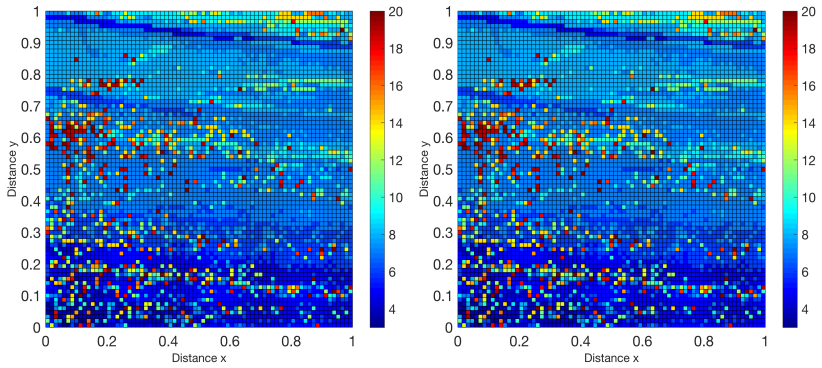

Figure 3: Optimal polynomial degree for the PCE method over each node of the computational mesh in the real part (left) and imaginary part (right) for plane wave propagation problem using $\overline{\kappa} = 2\pi$ and $CV = 10$ %.

a comparison of computational costs needed for the construction of PCE and POD-PCE surrogate models for uncertainty quantification in this test example using three values for the coefficient of variation CV. It is evident that increasing the amount of uncertainty in the problem results in an increase of CPU time for both methods. However, the computational costs required for the proposed POD-PCE approach is far lower than those required for the PCE method. For all considered values of CV, the POD-PCE method is more than 136 times computationally faster than the PCE method. The next set of results is dedicated to demonstrate that the reduction does not impact the accuracy of UQ.

In Figure 2 we present solutions for the mean wave potential obtained for the stochastic simulation along with the deterministic exact solution using the coefficient of variance $CV = 10$ %. For comparison reasons, we also include in this figure the difference between the two solutions. Note that, since the solution of the acoustic problems (1)-(2) are complex, we display results for both real and imaginary parts in our simulations. It is clear from the results presented in Figure 2 that, for the considered amount of uncertainty in the problem under study, the deterministic and the stochastic mean solutions exhibit similar trends.

The finite element method accurately resolves this stochastic wave problem and it reproduces numerical results free from any non-physical oscillations. It should be pointed out that, the PCE approach is implemented using the conventional techniques such that a suitable polynomial degree is determined for each node in the computational mesh. To illustrate this selection, Figure 3 presents the distribution of polynomial degrees in the finite element mesh for the real and imaginary parts of the solution. Under the considered stochastic inputs, the uncertainty is captured with polynomial degrees varying from 5 to 10. However, for some regions in the spatial domain (especially in the left side), the PCE method needed higher polynomial degrees. For such polynomial degrees, the order of magnitude for ϵ_{LOO} is 10^{-5} and 10^{-9} for the real part and imaginary part, respectively. These low values of the error ϵ_{LOO} confirm the convergence of the PCE method for this test example.

Next we compare the results obtained using the conventional PCE method applied to the full model and the POD-PCE method solving the reduced model. In this case, using a truncation criterion with $\epsilon = 10^{-4}$, only the first 8 eigenvalues are retained in the model and the PCE step is performed for each of mode. Therefore, the surrogate model needs only 8 decompositions instead of the 5776 decompositions representing the total number of nodes in the numerical model. The accuracy of the PCE method for each eigenvalues is assessed in Figure 4. In this figure we present the optimal polynomial degrees to estimate each spectral mode in the POD method and the *LOO*-error in the estimation of PCE method over each mode for both real and imaginary parts of the numerical solution. The results show a good convergence in the decomposition making them reliable for the UQ since the order of magnitude of the *LOO*-error is very low in the presented results.

Next, we compare in Figure 5 the numerical results obtained for the mean solutions using the MC, PCE and POD-PCE methods for both real and imaginary parts of the acoustic solutions. The results obtained for the variance are depicted in Figure 7. For a better insight, we display in Figure 9 horizontal cross-sections of the variance at $y = 0.45$. It is clear that from the obtained

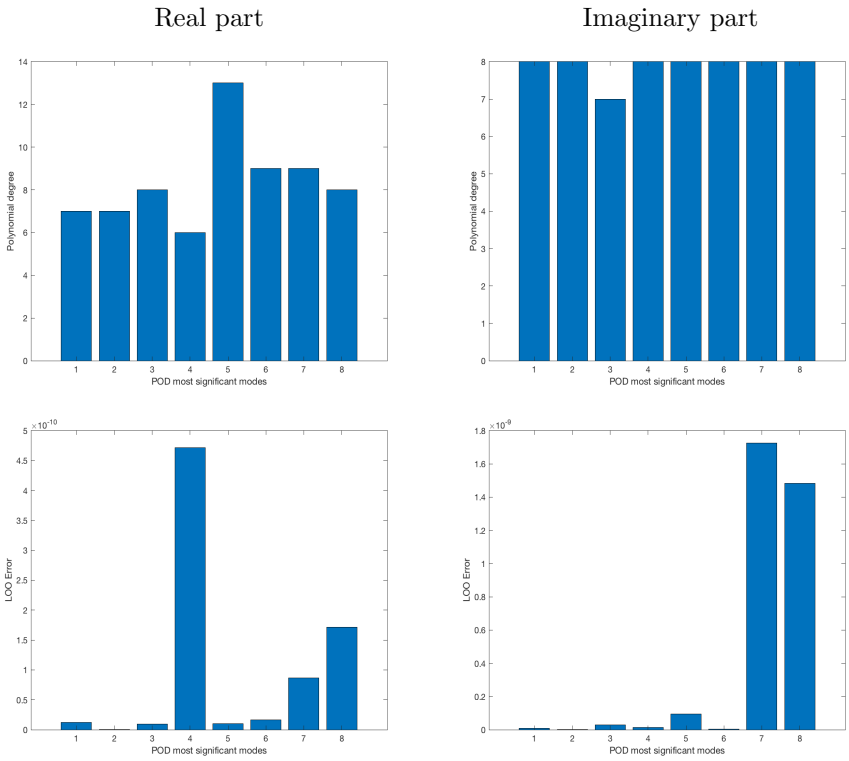

Figure 4: Optimal polynomial degrees to estimate each spectral mode in the POD method (first row) and *LOO*-error in the estimation of PCE method over each mode (second row) for the test example of plane wave propagation using $\overline{\kappa} = 2\pi$.

results for mean and variance that the three considered methods show the same wave patterns and capture the correct acoustic for this test case. For better insights, the L^2-error in the estimation of the first considered statistical moments, namely the mean and the variance are depicted in Figure 6 and Figure 8, respectively. It is evident that, as the magnitude of the error is very low ($< 10^{-4}$), one can state that both surrogate models efficiently capture the uncertainty displayed over the physical domain for the considered acoustic problem. However, this accuracy is achieved in the proposed POD-PCE method requiring very low computational cost compared to the MC and PCE methods.

We now turn our attention to the numerical case with a relatively high

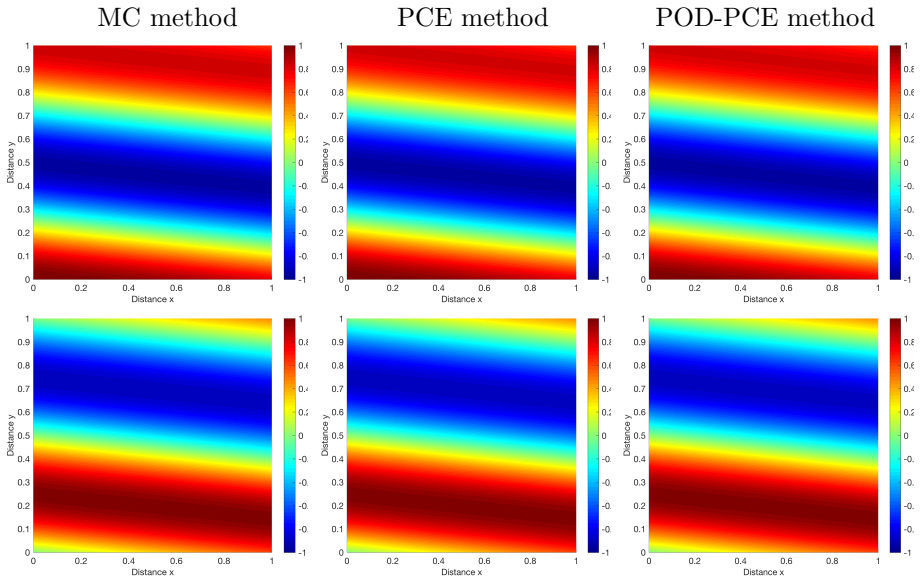

Figure 5: Mean solutions obtained using MC, PCE and POD-PCE methods for the real part (top) and imaginary part (bottom) for plane wave propagation problem using $\overline{\kappa} = 2\pi$.

wavenumber $\overline{\kappa} = 4\pi$. We carry out the same comparative study as in the previous test case for the plane wave propagation problem. Here, the unit squared domain is discretized into 1600 bilinear elements with 1681 nodes. Table 2 summarizes the computational costs needed by the PCE and POD-PCE methods for uncertainty quantification in this test example using three values for the coefficient of variation CV. Again, since the proposed POD-PCE method significantly reduces the computational model, it outperforms the classical PCE method. For the considered coefficient of variations, the POD-PCE method is about 35 times faster than the PCE method. This demonstrates the efficiency of the POD-PCE method for solving stochastic problems for wave acoustics with high wavenumbers.

Figure 10 presents the obtained mean solutions for the stochastic problem for the plane wave propagation problem using $CV = 15$ %. For comparison purposes, we also include the real and imaginary solutions for the deterministic problem. In the contrary to the first test example, the increase of the wavenum-

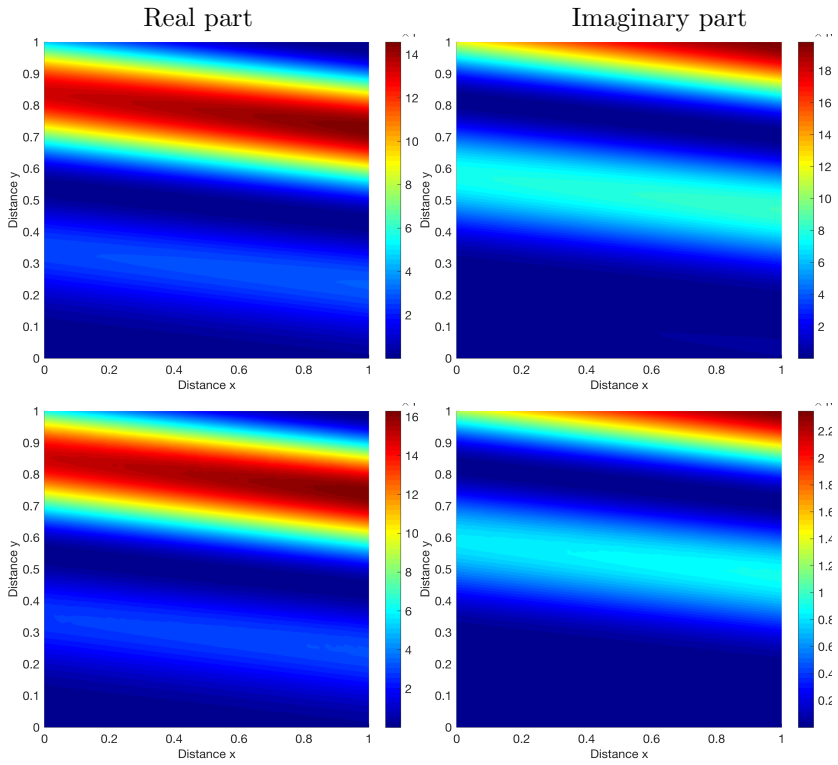

Figure 6: L^2-error in the estimation of the mean field using PCE method (first row) and POD-PCE method (second row) for the test example of plane wave propagation using $\overline{\kappa} = 2\pi$.

ber has resulted in an increase in the non-linearity of the problem. Therefore, the deterministic and the mean solutions are not exactly the same as notable in Figure 10. However, the wave patterns for $\overline{\kappa} = 4\pi$ have been preserved in the stochastic model and the diffusion is more pronounced that in their deterministic counterparts. As in the previous test case, we illustrate in Figure 11 the sensitivity of polynomial degrees for the real and imaginary parts of the solution in the computational mesh. An examination of the distributions in this figure reveals the non-linearity of the problem as high polynomial degrees are needed to capture the uncertainty. Here, under the considered stochastic inputs, the uncertainty is captured with polynomial degrees varying from 5 to 15. For such polynomial degrees, the order of magnitude for ϵ_{LOO} is 10^{-6} for

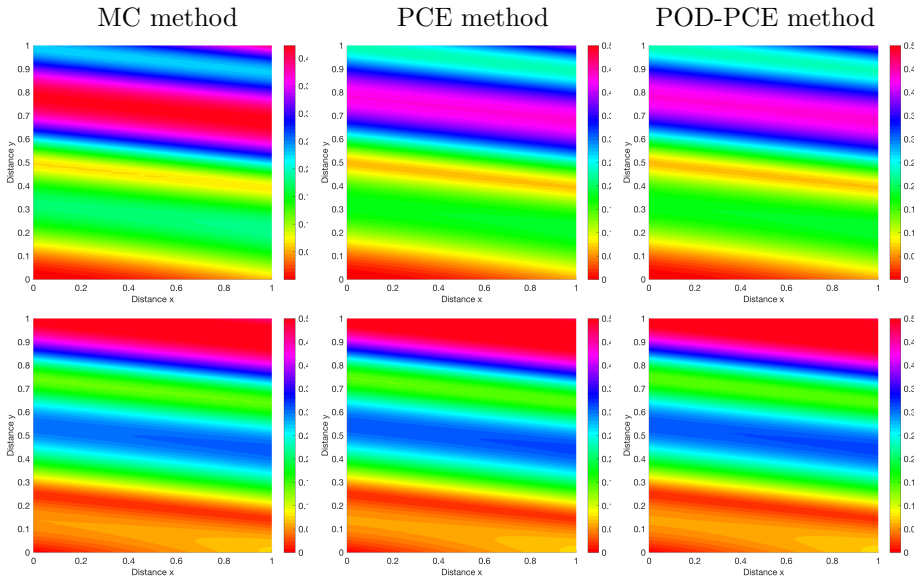

Figure 7: Same as Figure 5 but for the variance.

the both real and imaginary parts. This behavior confirms the convergence of the PCE method for this test case in plane wave propagations.

A comparison between the conventional PCE method applied to the full model and the POD-PCE method solving the reduced model has also been performed for this test example. Note that, as the non-linearity increases, the needed number of POD modes in the method also increases. In this test case, using a truncation criterion with $\epsilon = 10^{-4}$, only 14 eigenvalues are retained in the model and the PCE step is performed for each of mode. Thus, the surrogate model needs only 14 decompositions instead of the 1681 decompositions representing the total number of nodes in the numerical model. Figure 12 depicts the accuracy of the PCE method achieved for each eigenvalue. We present the optimal polynomial degrees to estimate each spectral mode in the POD method and the *LOO*-error in the estimation of PCE method over each mode for both real and imaginary parts of the numerical solution. The results also show a good convergence in the decomposition making them reliable for UQ as the order of

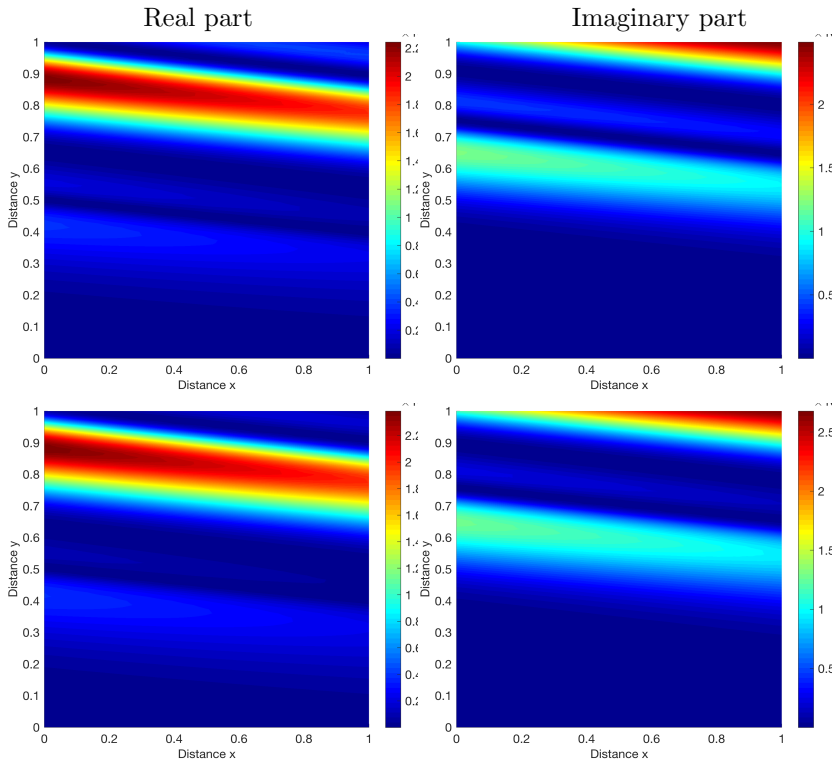

Figure 8: L^2-error in the estimation of the variance field using PCE method (first row) and POD-PCE method (second row) for the test example of plane wave propagation using $\overline{\kappa} = 2\pi$.

magnitude of the *LOO*-error is very low in the computed results.

As a final comment on this test example, we present in Figure 13 a comparison between the numerical results obtained for the mean solutions using the MC, PCE and POD-PCE methods for both real and imaginary parts of the solutions. The comparative results obtained for the variance are depicted in Figure 14. To further illustrate this comparison we display in Figure 9 the horizontal cross-sections of the variance solutions at $y = 0.45$. For this case with $\overline{\kappa} = 4\pi$, the conventional PCE method is not able to exactly reproduce the variance field. Indeed, the PCE method offers tools that allow to represent global UQ for a localized random variable. Therefore, the uncertainty that propagates through the spatial domain is not well-represented using the PCE method. On

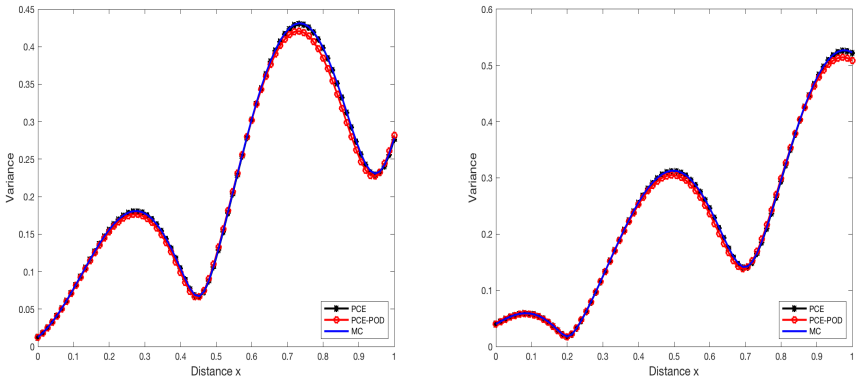

Figure 9: Cross-sections of the variance solutions in Figure 7 for the real part (left) and imaginary part (right) for plane wave propagation problem using $\overline{\kappa} = 2\pi$.

Table 2: CPU times (in seconds) required by PCE and POD-PCE methods for solving plane wave propagation problem using $\overline{\kappa} = 4\pi$. Numbers in parenthesis refer to the number of modes used in the POD-PCE method for a threshold of $\epsilon = 10^{-4}$. The results are obtained for an equivalent accuracy in both methods.

CV	PCE method	POD-PCE method
5 %	2250	53 (8)
10 %	2673	90 (13)
15 %	3268	93 (14)

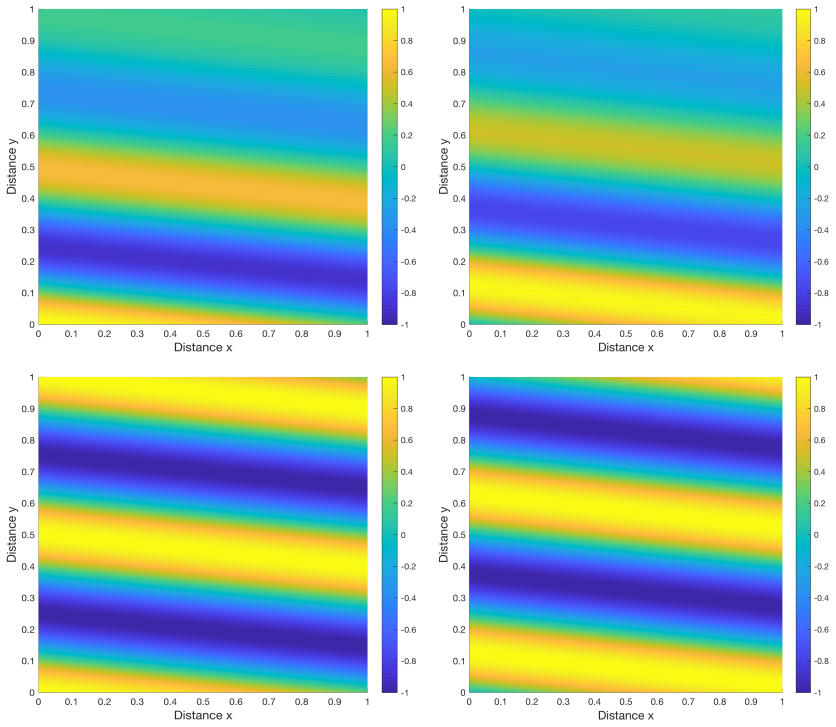

Figure 10: Mean wave potential $\overline{u(x, y, \zeta_\kappa, \zeta_\alpha)}$ obtained for the stochastic simulation (first row) and the deterministic exact solution $u(x, y)$ (second row) obtained for plane wave propagation problem using $\overline{\kappa} = 4\pi$ and $CV = 15$ %. We present results for the real part (left) and imaginary part (right).

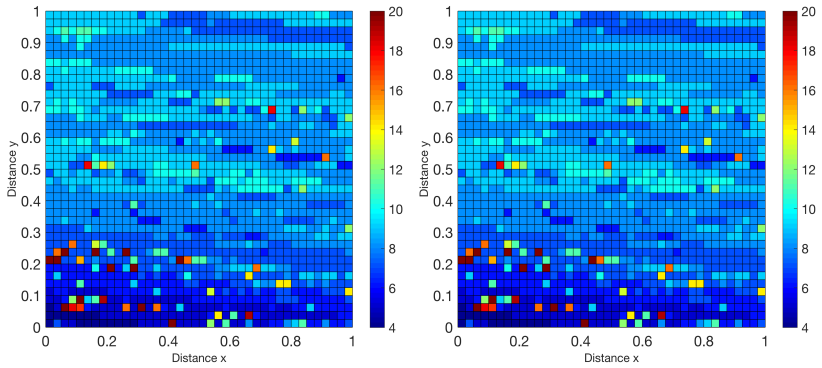

Figure 11: Optimal polynomial degree for the PCE method over each node of the computational mesh in the real part (left) and imaginary part (right) for plane wave propagation problem using $\overline{\kappa} = 4\pi$ and $CV = 15\ \%$.

the other hand, the POD-PCE method propagates the uncertainty over each eigenmode. These latter contain already the spatial dependence and therefore, when executing a PCE step over an eigenvalue the method captures the necessary information and it reproduces the uncertainty correctly. In summary, from a computational and UQ point of views, the POD-PCE method is more efficient and accurate than the classical PCE method for numerical outputs in the form of stochastic processes in plane waves.

4.2. Plane wave scattering

Our second test example consists of a plane wave scattering by a circular cylinder studied for example in [78, 22]. If the incident wave propagates in the negative x-axis direction then the scattered wave field can be evaluated analytically using the expression

$$u = -\sum_{n=0}^{\infty} \mathrm{i}\epsilon_n \frac{J_n'(ka)}{H_n'(\kappa a)} H_n(\kappa r)\cos(n\theta), \tag{24}$$

where $\epsilon_n = 1$ for $n = 0$ and $\epsilon_n = 2$ for $n \neq 0$ while $J_n(\kappa a)$ is the well-established Bessel and $H_n(\kappa a)$ is Hankel function of the first kind and order n. The prime denotes the derivative of a function with respect to its argument. Note that the expression (24) is written in polar coordinate r and θ whereas, the scatter

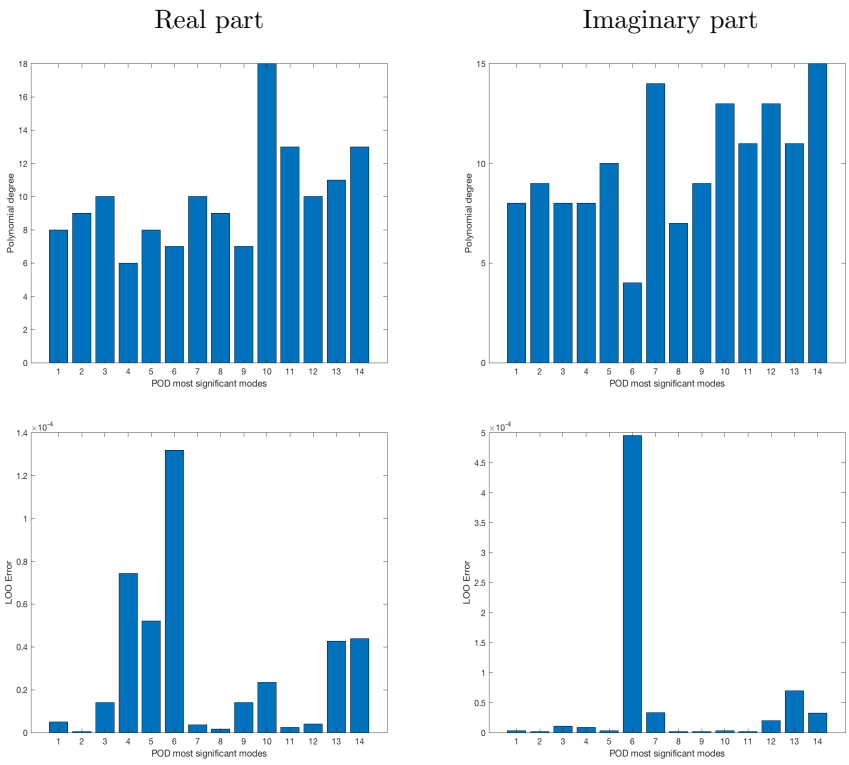

Figure 12: Optimal polynomial degrees to estimate each spectral mode in the POD method (first row) and *LOO*-error in the estimation of PCE method over each mode (second row) for the test example of plane wave propagation using $\overline{\kappa} = 4\pi$.

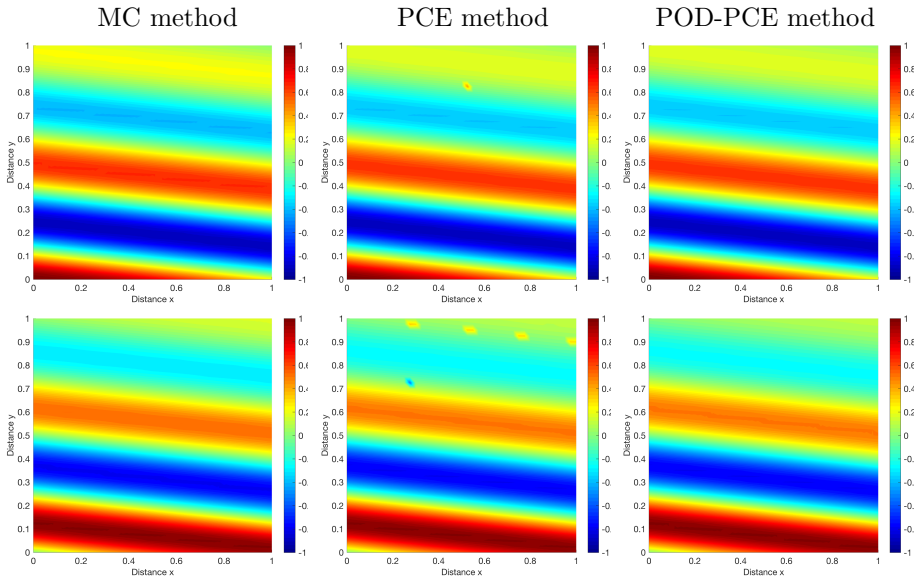

Figure 13: Mean solutions obtained using MC, PCE and POD-PCE methods for the real part (top) and imaginary part (bottom) for plane wave propagation problem using $\overline{\kappa} = 4\pi$.

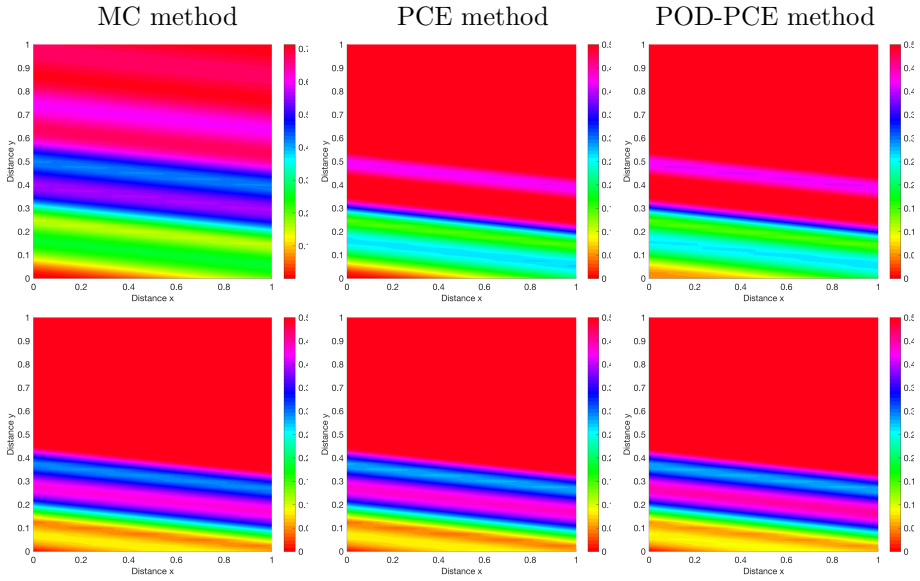

Figure 14: Same as Figure 13 but for the variance.

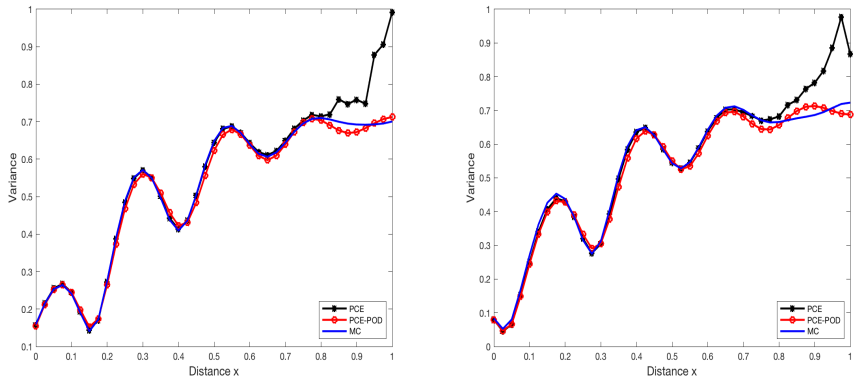

Figure 15: Cross-sections of the variance solutions in Figure 14 for the real part (left) and imaginary part (right) for plane wave propagation problem using $\overline{\kappa} = 4\pi$.

radius is a. In this test example the domain Ω is taken to be annular defined with the inner and outer radii *i.e.* $r_i = 1$ and $r_o = 2$, respectively. The analytical expression (24) of the scattered wave is imposed on the domain inner and outer boundaries using Robin-type boundary condition (2). The objective of this test examples if to examine the ability of the proposed POD-PCE method for recovering the pressure of a plane wave scattered by an infinity rigid circular scatterer subject to stochastic wavenumbers. In this example only the wavenumber is considered to be stochastic in the form of (23) with a mean value $\overline{\kappa} = 4\pi$ and coefficient of variation $CV = 10$ %. A finite element mesh formed of 4-noded bilinear elements with a total number of 9375 elements and 9500 nodes is used in our simulations. For the selected conditions, the CPU time needed for the PCE method and POD-PCE method is 1260 and 28 seconds, respectively. This confirms the efficiency of the proposed POD-PCE to resolve this problem of plane wave scattering.

In Figure 16 we present solutions for the mean wave potential obtained for the stochastic simulation along with the deterministic solution. As can be seen, there is a slight difference between the two solution fields in the magnitude order mainly due to non-linearity raised by incorporation of stochastic effect in the

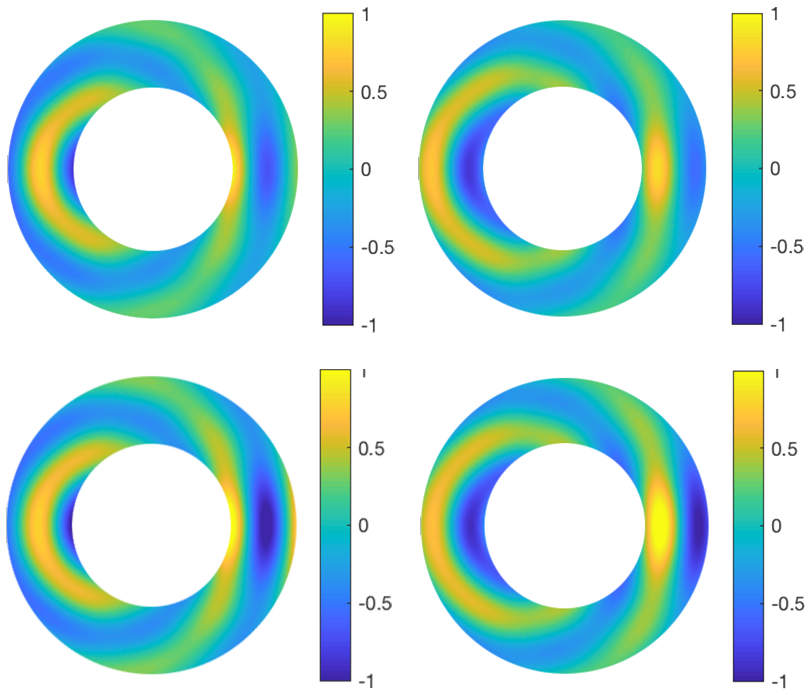

Figure 16: Mean wave potential $\overline{u(r,\theta,\zeta_\kappa)}$ obtained for the stochastic simulation (first row) and the deterministic solution $u(r,\theta)$ (second row) obtained for plane wave scattering problem using $\overline{\kappa} = 4\pi$ and $CV = 10$ %. We present results for the real part (left) and imaginary part (right).

wave number. It is also clear that the finite element method accurately resolves this stochastic wave problem as no non-physical oscillations are detected in the computational results. As in the previous test example, we also illustrate in Figure 17 the distribution of optimal polynomial degrees in the finite element mesh for the real and imaginary parts of the numerical solution. Obviously, the spatial domain needs more polynomial degree to resolve all the uncertainty as in some nodes the degree varies between 15 to 20. The average error for PCE method in this situation is of the order of 10^{-6}. Using the same value of the POD truncation criterion with $\epsilon = 10^{-4}$ as in the previous simulations, a set of 7 eigenmodes is sufficient to reduce the physical model. Thus, the surrogate model for plane wave scattering needs only 7 decompositions instead of the 9500

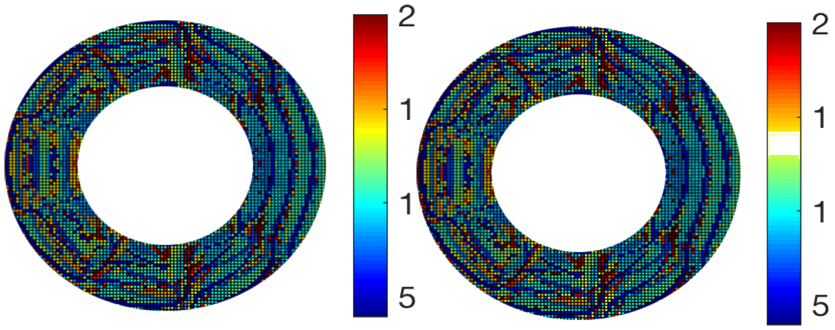

Figure 17: Optimal degree for PCE over each node of the mesh.

decompositions representing the total number of nodes in the numerical model. Figure 18 illustrates the accuracy of the PCE method for each eigenvalue in the model. We present the optimal polynomial degrees to estimate each spectral mode in the POD method and the *LOO*-error in the estimation of PCE method over each mode for both real and imaginary parts of the numerical solution. Again, the presented results show a good convergence in the decomposition making them reliable for UQ as the order of magnitude of the *LOO*-error is very low in the computed results.

Finally, Figure 19 presents a comparison between the numerical results obtained for the mean solutions using the MC, PCE and POD-PCE methods for both real and imaginary parts of the solutions. Those comparative results obtained for the variance are shown in Figure 20. For the considered wave conditions, the three method exhibit similar acoustic trends around the scatter. Bearing in mind the low computational effort required for the PCE-POD method, this latter could be considered as an ideal algorithm for UQ in computational acoustic with stochastic inputs.

5. Conclusions

In the present study, an efficient analysis of uncertainty quantification for acoustic problems with large number of random variables related to the wavenum-

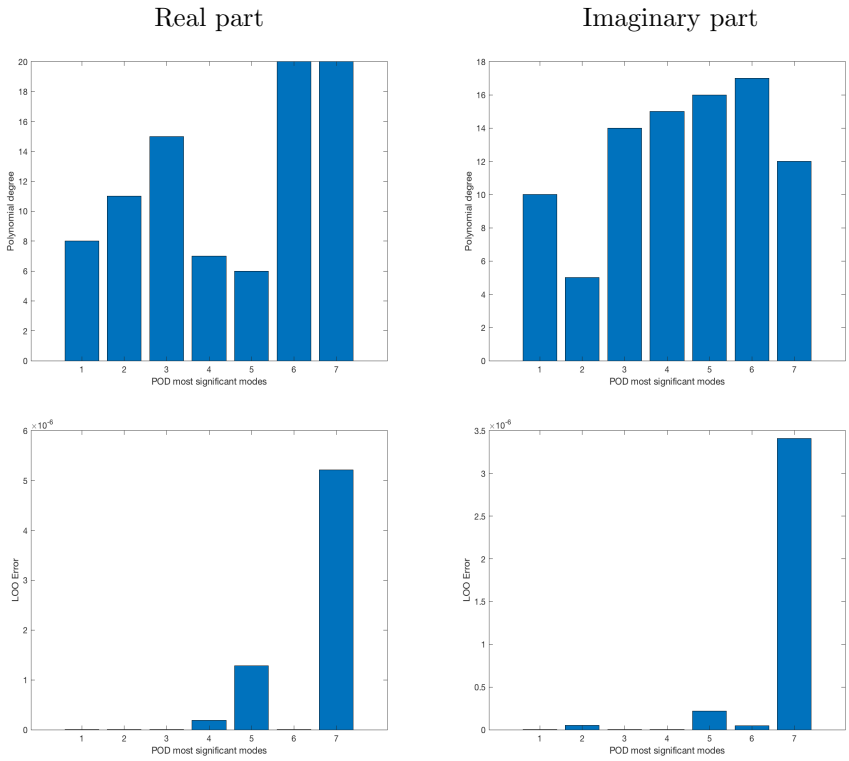

Figure 18: Optimal polynomial degree to estimate each spectral mode in the POD (first row) and *LOO*-error in the estimation of PCE over each mode (second row) for the test example of plane wave scattering using $\kappa = 4\pi$.

bers is presented and discussed. The reduced-order model is applied to the two-dimensional Helmholtz equation using a finite element method. In all test examples, uncertainty quantification is performed using both the full polynomial chaos expansion and the combination of full polynomial chaos expansion with proper orthogonal decomposition. Distributions of mean and variance obtained from the reduced-order model are compared to those computed using the full-order model. The numerical results show that the developed reduced-order model is able to produce acceptable results for such statistical quantities.

It should be stressed that although we have concentrated here on the uncertainty associated with the wavenumber but solving wave problems also involves

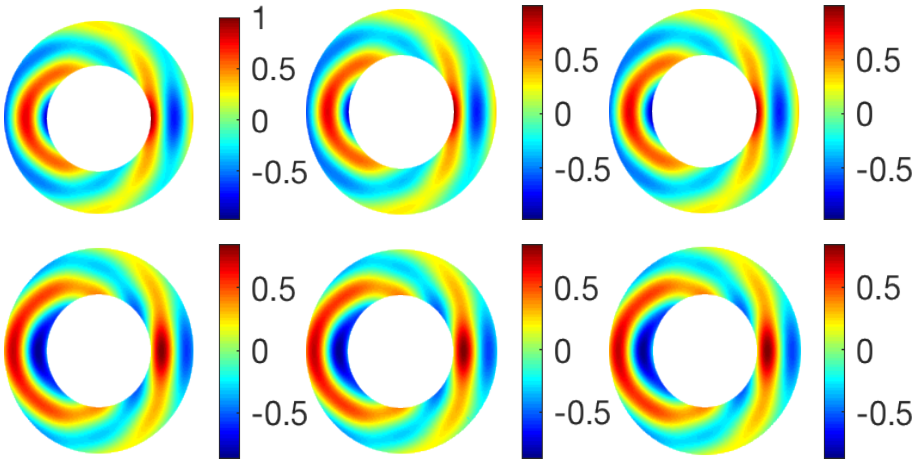

Figure 19: Mean solutions obtained using MC, PCE and POD-PCE methods for the real part (top) and imaginary part (bottom) for plane wave scattering problem using $\overline{\kappa} = 4\pi$.

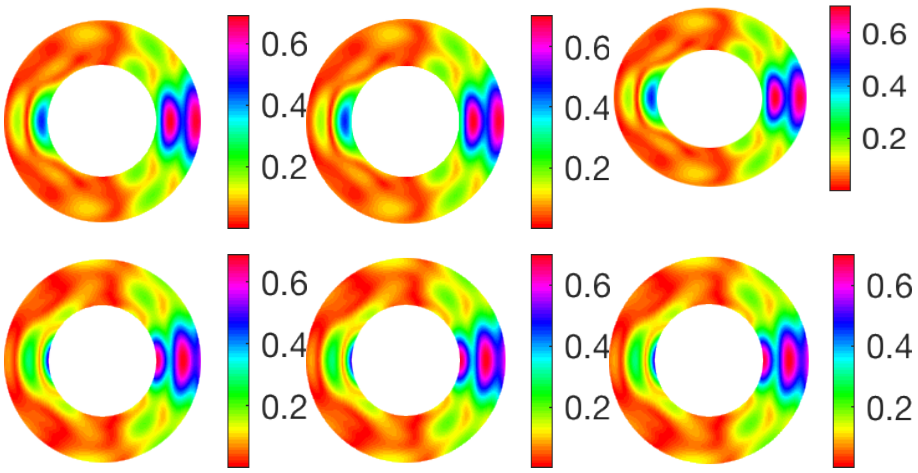

Figure 20: Same as Figure 19 but for the variance.

other uncertainties coming from approximations of the geometry as well as the boundary conditions. Furthermore, the current work investigates problems at relatively low wavenumbers. Considering high wavenumbers involves difficulties related to the stability of the finite element method as well as the intensive

computations involved in generating enough samples for the stochastic analysis. These are some of the issues that we aim to investigate in future works.

Acknowledgment. The authors would like to thank anonymous referees for giving very helpful comments and suggestions that have greatly improved this paper.

References

[1] S. Kawamoto, Y. Ohta, Y. Hiyama, M. Todoriki, T. Nishimura, T. Furuya, Y. Sato, T. Yahagi, K. Miyagawa, Regard: A new gnss-based real-time finite fault modeling system for geonet, Journal of Geophysical Research: Solid Earth 122 (2017) 1324–1349.

[2] G.-Y. Hwang, S.-M. Hwang, H.-J. Lee, J.-H. Kim, K.-S. Hong, W.-Y. Lee, Application of taguchi method to robust design of acoustic performance in IMT-2000 mobile phones, IEEE transactions on magnetics 41 (2005) 1900–1903.

[3] H. H. Zhang, P. Yuan, P. Y. Chen, W. W. Choi, Simulation of temperature increase of human head model exposed to cell phones, in: 2018 International Applied Computational Electromagnetics Society Symposium-China (ACES), IEEE, 2018, pp. 1–2.

[4] S. Frisken, M. Luo, I. Machado, P. Unadkat, P. Juvekar, A. Bunevicius, M. Toews, W. Wells, M. I. Miga, A. J. Golby, Preliminary results comparing thin-plate splines with finite element methods for modeling brain deformation during neurosurgery using intraoperative ultrasound, in: Medical Imaging 2019: Image-Guided Procedures, Robotic Interventions, and Modeling, Vol. 10951, International Society for Optics and Photonics, 2019, p. 1095120.

[5] M. K. Chung, J. Taylor, Diffusion smoothing on brain surface via finite element method, in: 2004 2nd IEEE International Symposium on Biomed-

ical Imaging: Nano to Macro (IEEE Cat No. 04EX821), IEEE, 2004, pp. 432–435.

[6] A. Heidari, M. Guddati, Novel finite-element-based subsurface imaging algorithms, Finite elements in analysis and design 43 (2007) 411–422.

[7] S. Nounouh, C. Eyraud, A. Litman, H. Tortel, Near-subsurface imaging in an absorbing embedding medium with a multistatic/single frequency scanner, Near Surface Geophysics 13 (2015) 211–218.

[8] C. Key, A. Smull, B. M. Notaroš, D. Estep, T. Butler, Adjoint methods for uncertainty quantification in applied computational electromagnetics: FEM scattering examples, in: 2018 International Applied Computational Electromagnetics Society Symposium (ACES), IEEE, 2018, pp. 1–2.

[9] P. Zakian, N. Khaji, A stochastic spectral finite element method for wave propagation analyses with medium uncertainties, Applied Mathematical Modelling (2018) 84–108.

[10] F. Sahraoui, G. Belmont, M. Goldstein, L. Rezeau, Limitations of multispacecraft data techniques in measuring wave number spectra of space plasma turbulence, Journal of Geophysical Research: Space Physics 115 (A4).

[11] V. Resseguier, E. Mémin, B. Chapron, Geophysical flows under location uncertainty, part III SQG and frontal dynamics under strong turbulence conditions, Geophysical & Astrophysical Fluid Dynamics 111 (2017) 209–227.

[12] R. Ghanem, D. Higdon, H. Owhadi, Handbook of uncertainty quantification, Vol. 6, Springer, 2017.

[13] D. Xiu, Numerical Methods for Stochastic Computations: A Spectral Method Approach, Princeton University Press, 2010.

[14] G. Poëtte, A. Birolleau, D. Lucor, Iterative Polynomial Approximation Adapting to Arbitrary Probability Distribution, SIAM J. Numerical Analysis 53 (2015) 1559–1584.

[15] N. El Moçayd, La décomposition en polynôme du chaos pour l'amélioration de l'assimilation de données ensembliste en hydraulique fluviale, Ph.D. thesis (2017).

[16] B. Després, G. Poëtte, D. Lucor, Robust uncertainty propagation in systems of conservation laws with the entropy closure method, in: Uncertainty quantification in computational fluid dynamics, Springer, 2013, pp. 105–149.

[17] J. Tryoen, O. Le Maitre, M. Ndjinga, A. Ern, Intrusive Galerkin methods with upwinding for uncertain nonlinear hyperbolic systems, Journal of Computational Physics 229 (2010) 6485–6511.

[18] A. Nouy, A generalized spectral decomposition technique to solve a class of linear stochastic partial differential equations, Computer Methods in Applied Mechanics and Engineering 196 (2007) 4521–4537.

[19] M. T. Reagana, H. N. Najm, R. G. Ghanem, O. M. Knio, Uncertainty quantification in reacting-flow simulations through non-intrusive spectral projection, Combustion and Flame 132 (2003) 545–555.

[20] L. Gilli, D. Lathouwers, J. Kloosterman, T. Van der Hagen, A. Koning, D. Rochman, Uncertainty quantification for criticality problems using non-intrusive and adaptive polynomial chaos techniques, Annals of Nuclear Energy 56 (2013) 71–80.

[21] G. Poëtte, D. Lucor, Non intrusive iterative stochastic spectral representation with application to compressible gas dynamics, Journal of Computational Physics 231 (2012) 3587–3609.

[22] G. C. Diwan, M. S. Mohamed, Pollution studies for high order isogeometric analysis and finite element for acoustic problems, Computer Methods in Applied Mechanics and Engineering 350 (2019) 701–718.

[23] J. Cheng, J. Wang, X. Wu, S. Wang, An improved polynomial-based nonlinear variable importance measure and its application to degradation assessment for high-voltage transformer under imbalance data, Reliability Engineering & System Safety 185 (2019) 175–191.

[24] J. A. Vrugt, B. A. Robinson, Treatment of uncertainty using ensemble methods: Comparison of sequential data assimilation and Bayesian model averaging, Water Resources Research 43.

[25] R. Schefzik, T. L. Thorarinsdottir, T. Gneiting, et al., Uncertainty quantification in complex simulation models using ensemble copula coupling, Statistical science 28.

[26] G. Saad, R. Ghanem, Characterization of reservoir simulation models using a polynomial chaos-based ensemble kalman filter, Water Resources Research 45.

[27] C. J. Geyer, On the convergence of Monte Carlo maximum likelihood calculations, Journal of the Royal Statistical Society: Series B (Methodological) 56 (1994) 261–274.

[28] R. Faivre, B. Iooss, S. Mahévas, D. Makowski, H. Monod, Analyse de sensibilité et exploration de modèles: application aux sciences de la nature et de l'environnement, Editions Quae, 2016.

[29] B. Sudret, Meta-models for structural reliability and uncertainty quantification, arXiv preprint arXiv:1203.2062.

[30] M. Berveiller, B. Sudret, M. Lemaire, Stochastic finite element: a non intrusive approach by regression, European Journal of Computational Mechanics/Revue Européenne de Mécanique Numérique 15 (2006) 81–92.

[31] M. M. Rajabi, Review and comparison of two meta-model-based uncertainty propagation analysis methods in groundwater applications: polynomial chaos expansion and Gaussian process emulation, Stochastic Environmental Research and Risk Assessment (2019) 1–25.

[32] P. Kersaudy, B. Sudret, N. Varsier, O. Picon, J. Wiart, A new surrogate modeling technique combining kriging and polynomial chaos expansions–application to uncertainty analysis in computational dosimetry, Journal of Computational Physics 286 (2015) 103–117.

[33] O. G. Ernst, A. Mugler, H.-J. Starkloff, E. Ullmann, On the convergence of generalized polynomial chaos expansions, ESAIM: Mathematical Modelling and Numerical Analysis 46 (2) (2012) 317–339.

[34] P. T. Roy, N. El Moçayd, S. Ricci, J.-C. Jouhaud, N. Goutal, M. De Lozzo, M. C. Rochoux, Comparison of polynomial chaos and Gaussian process surrogates for uncertainty quantification and correlation estimation of spatially distributed open-channel steady flows, Stochastic Environmental Research and Risk Assessment (2017) 1–19.

[35] C. Rasmussen, C. Williams, Gaussian processes for machine learning the mit press (2006).

[36] P. Spanos, R. Ghanem, Stochastic Finite Elements: A Spectral Approach, Springer, 1991.

[37] R. H. Cameron, W. T. Martin, The orthogonal development of non-linear functionals in series of fourier-hermite functionals, Annals of Mathematics (1947) 385–392.

[38] D. Xiu, G. E. Karniadakis, The wiener–askey polynomial chaos for stochastic differential equations, SIAM Journal on Scientific Computing 24 (2002) 619–644.

[39] R. Askey, J. A. Wilson, Some basic hypergeometric orthogonal polynomials that generalize Jacobi polynomials, Vol. 319, American Mathematical Soc., 1985.

[40] M. C. Rochoux, S. Ricci, B. Lucor, D.and Cuenot, A. Trouvé, Towards predictive data-driven simulations of wildfire spread - Part 1: Reduced-cost Ensemble Kalman Filter based on a Polynomial Chaos surrogate model for parameter estimation, Nat. Hazards and Earth Syst. Sci. (11) (2014) 2951–2973.

[41] Y. Wang, K. Hu, L. Ren, G. Lin, Optimal observations-based retrieval of topography in 2D shallow water equations using PC-enkf, Journal of Computational Physics 382 (2019) 43–60.

[42] M. El-Amrani, M. Seaid, A spectral stochastic semi-Lagrangian method for convection-diffusion equations with uncertainty, Journal of Scientific Computing 39 (2009) 371–393.

[43] M. El-Amrani, M. Seaid, M. Zahri, A stabilized finite element method for stochastic incompressible Navier-Stokes equations, International Journal of Computer Mathematics 89 (2012) 2576–2602.

[44] G. Blatman, B. Sudret, Adaptative sparse polynomial chaos expansion based on Least Angle Regression, Journal of Computational Physics 230 (2011) 2345–2367.

[45] B. Efron, T. Hastie, I. Johnstone, R. Tibshirani, Least angle regression, The Annals of Statistics 32 (2004) 407–499.

[46] R. Schobi, B. Sudret, J. Wiart, Polynomial-chaos-based kriging, International Journal for Uncertainty Quantification 5.

[47] N. El Moçayd, S. Ricci, N. Goutal, M. C. Rochoux, S. Boyaval, C. Goeury, D. Lucor, O. Thual, Polynomial surrogates for open-channel flows in random steady state, Environmental Modeling & Assessment 23 (2018) 309–331.

[48] W. Yamazaki, T. Kato, T. Homma, K. Shimoyama, S. Obayashi, Stochastic tsunami inundation flow simulation via polynomial chaos approach, Journal of Fluid Science and Technology (4) (2018) JFST0025–JFST0025.

[49] C. Salis, T. Zygiridis, Dimensionality reduction of the polynomial chaos technique based on the method of moments, IEEE Antennas and Wireless Propagation Letters 17 (12) (2018) 2349–2353. doi:10.1109/LAWP.2018.2874521.

[50] C. Schwab, R. A. Todor, Karhunen–loève approximation of random fields by generalized fast multipole methods, Journal of Computational Physics 217 (2006) 100–122.

[51] Y. M. Marzouk, H. N. Najm, Dimensionality reduction and polynomial chaos acceleration of Bayesian inference in inverse problems, Journal of Computational Physics 228 (2009) 1862–1902.

[52] G. Perrin, Random fields and associated statistical inverse problems for uncertainty quantification: application to railway track geometries for high-speed trains dynamical responses and risk assessment, Ph.D. thesis, Paris Est (2013).

[53] G. Blatman, B. Sudret, Principal component analysis and Least Angle Regression in spectral stochastic finite element analysis, in: M. Faber, J. Köhler, K. Nishijima (Eds.), Proc. 11th Int. Conf. on Applications of Stat. and Prob. in Civil Engineering (ICASP11), Zurich, Switzerland, 2011.

[54] M. Chevreuil, A. Nouy, Model order reduction based on proper generalized decomposition for the propagation of uncertainties in structural dynamics, International Journal for Numerical Methods in Engineering 89 (2012) 241–268.

[55] M. Raisee, D. Kumar, C. Lacor, A non-intrusive model reduction approach for polynomial chaos expansion using proper orthogonal decomposition,

International Journal for Numerical Methods in Engineering 103 (2015) 293–312.

[56] X. Zhang, N. Wang, F. Cao, J. Han, S. Lv, The fluctuation and uncertainty of acoustic measurement in shallow water wave-guide, in: 2016 IEEE/OES China Ocean Acoustics (COA), IEEE, 2016, pp. 1–5.

[57] I. Harari, T. J. Hughes, Finite element methods for the Helmholtz equation in an exterior domain: model problems, Computer methods in applied mechanics and engineering 87 (1991) 59–96.

[58] F. Ihlenburg, I. Babuška, Finite element solution of the Helmholtz equation with high wave number Part i: The h-version of the FEM, Computers & Mathematics with Applications 30 (1995) 9–37.

[59] F. Ihlenburg, I. Babuska, Finite element solution of the Helmholtz equation with high wave number part ii: the hp version of the FEM, SIAM Journal on Numerical Analysis 34 (1997) 315–358.

[60] T. Strouboulis, I. Babuška, R. Hidajat, The generalized finite element method for Helmholtz equation: theory, computation, and open problems, Computer Methods in Applied Mechanics and Engineering 195 (2006) 4711–4731.

[61] K. Christodoulou, O. Laghrouche, M. S. Mohamed, J. Trevelyan, High-order finite elements for the solution of Helmholtz problems, Computers & Structures 191 (2017) 129–139.

[62] K. Uenishi, T. Okuzono, K. Sakagami, Finite element analysis of absorption characteristics of permeable membrane absorbers array, Acoustical Science and Technology 38 (2017) 322–325.

[63] T. Okuzono, K. Sakagami, A time-domain finite element model of permeable membrane absorbers, Acoustical Science and Technology 37 (2016) 46–49.

[64] T. Okuzono, K. Sakagami, Room acoustics simulation with single-leaf microperforated panel absorber using two-dimensional finite-element method, Acoustical Science and Technology 36 (2015) 358–361.

[65] N. Wiener, The homogeneous chaos, Am.J.Math 60.

[66] D. Xiu, G. E. Karniadakis, Modeling uncertainty in flow simulations via generalized polynomial chaos, Journal of Computational Physics 187 (2003) 137–167.

[67] O. Le Maitre, O. Knio, Spectral Methods for Uncertainty Quantification, Springer, 2010.

[68] S.-K. Choi, R. V. Grandhi, R. A. Canfield, C. L. Pettit, Polynomial Chaos expansion with Latin Hypercube Sampling for estimating response variability, AIAA journal 42 (2004) 1191–1198.

[69] G. Casella, E. I. George, Explaining the Gibbs sampler, The American Statistician 46 (1992) 167–174.

[70] A. F. Smith, G. O. Roberts, Bayesian computation via the Gibbs sampler and related markov chain Monte Carlo methods, Journal of the Royal Statistical Society: Series B (Methodological) 55 (1993) 3–23.

[71] S. Bontemps, A. Kaemmerlen, G. Blatman, L. Mora, Reliability of dynamic simulation models for building energy in the context of low-energy buildings, Proceedings of BS2013 (2013) 1952–1959.

[72] M. Baudin, A. Dutfoy, B. Iooss, A.-L. Popelin, Openturns: An industrial software for uncertainty quantification in simulation, Handbook of uncertainty quantification (2017) 2001–2038.

[73] C. Goeury, T. David, R. Ata, S. Boyaval, Y. Audouin, N. Goutal, A.-L. Popelin, M. Couplet, M. Baudin, R. Barate, Uncertainty quantification on a real case with telemac-2D, in: Proceedings of the XXII TELEMAC-MASCARET Technical User Conference October 15-16, 2047, 2015, pp. 44–51.

[74] M. Drolia, M. S. Mohamed, O. Laghrouche, M. Seaid, J. Trevelyan, Enriched finite elements for initial-value problem of transverse electromagnetic waves in time domain, Computers & Structures 182 (2017) 354–367.

[75] S. Dubreuil, M. Berveiller, F. Petitjean, M. Salan, Construction of bootstrap confidence intervals on sensitivity indices computed by polynomial chaos expansion, Reliability Engineering and System Safety 121 (2014) 263 – 275.

[76] R. Crisovan, D. Torlo, R. Abgrall, S. Tokareva, Model order reduction for parametrized nonlinear hyperbolic problems as an application to uncertainty quantification, Journal of Computational and Applied Mathematics 348 (2019) 466–489.

[77] G. Blatman, B. Sudret, Sparse polynomial chaos expansions of vector-valued response quantities, in: G. Deodatis (Ed.), Proc. 11th Int. Conf. Struct. Safety and Reliability (ICOSSAR'2013), New York, USA, 2013.

[78] J. Jiang, M. S. Mohamed, M. Seaid, H. Li, Identifying the wavenumber for the inverse Helmholtz problem using an enriched finite element formulation, Computer Methods in Applied Mechanics and Engineering 340 (2018) 615–629.